BNL-68994-02/11-Rev.

CHEMICALLY-RESOLVED AEROSOL DYNAMICS FOR INTERNAL MIXTURES BY THE QUADRATURE METHOD OF MOMENTS

R. McGraw and D. L. Wright
Atmospheric Sciences Division
Environmental Sciences Department
Brookhaven National Laboratory
Upton, NY 11973-5000

November 2002

Accepted for publication in
Journal of Aerosol Science

Research by BNL investigators was performed under the auspices of the U.S. Department of Energy under Contract No. DE-AC02-98CH10886.

Chemically-resolved aerosol dynamics for internal mixtures by the quadrature method of moments

Robert McGraw and Douglas L. Wright

Environmental Sciences Department

Brookhaven National Laboratory, Upton NY 11973

Abstract

The quadrature method of moments (QMOM), a promising new tool for aerosol dynamics simulation, is extended to multicomponent, internally-mixed particle populations. A new moment closure method, the Jacobian matrix transformation (JMT), is introduced and shown to provide an efficient procedure for evolving quadrature abscissas and weights directly and in closed form. For special growth laws where analytic results are available for comparison, the QMOM is also found to be exact. The JMT implementation of the QMOM is used to explore the asymptotic behavior of coagulating aerosols at long time. Nondimensional reduced moments are constructed, and found to evolve to constant values in excellent agreement with estimates derived from 'self-preserving' distributions previously obtained by independent methods. Our findings support the QMOM as a new tool for rapid, accurate simulation of the dynamics of an evolving internally-mixed aerosol population, including the approach to asymptotic behavior at long time, in terms of lower-order moments.

Keywords: aerosol dynamics, moment methods, coagulation, self-preserving distributions

Accepted for publication in the Journal of Aerosol Science (2002)

1. Introduction

The accurate and efficient representation of aerosol microphysical processes is a growing requirement in such diverse modeling applications as combustion, nano-particle synthesis, and assessment of radiative and chemical effects of natural and anthropogenic atmospheric aerosols and their impact on climate. Most aerosol models explicitly represent the particle size distribution using either discrete bins (the sectional approach) or assumed functional forms for various modes of the distribution (the modal approach). These are standard modeling schemes well-investigated in the literature. More recently there have been advances in representing aerosols by the moments of the size distribution rather than the distribution itself. This approach, the method of moments (MOM), offers significant advantages for incorporating aerosol processes in large-scale models, provided closed sets of dynamical equations for evolution of the moments can be obtained (Friedlander, 1983; McGraw and Saunders, 1984; Pratsinis, 1988; McGraw, 1997). These include comparatively straightforward implementation of the method as the moments evolve according to (closed) sets of differential equations having the structure of typical rate equations governing the evolution of reacting chemical species in the same background flow. Additionally, simulations of aerosol dynamics based on moments are free from uncertainties associated with numerical diffusion (in particle size space) and tend to have greatly superior computational speed when compared with the sectional approach (Frenklach and Harris, 1987).

Closure of the moment evolution equations has always been the key issue. The conditions necessary for exact closure are encountered only in highly specialized cases such as free-molecular growth (Hulburt and Katz, 1964). However with the recent introduction of the quadrature method of moments (QMOM) (McGraw, 1997; Barrett and Webb, 1998), condensation and coagulation kernels of arbitrary form can be treated without the need for a priori assumptions about the size distribution. Thus the QMOM has become a viable candidate for modeling aerosols under very general conditions. The first paper (McGraw, 1997) introduced the quadrature-based closure technique and its application to arbitrary rate

laws for evaporation and condensation growth. In essence, the QMOM replaces exact closure with an approximate, but much less restrictive closure condition, while enabling evaluation of physical and optical properties as integrals over a particle distribution function when only the lower-order moments of the distribution are known. The method has been applied to coagulation and condensation (Barrett and Webb, 1998) and more recently - with nucleation, condensation, and coagulation all included within the QMOM framework - to the representation of aerosols in a sub-hemispheric scale atmospheric chemical transport and transformation model (Wright et al. 2000).

The present paper continues development of the QMOM through its extension to internally-mixed multicomponent aerosols undergoing growth by condensation and coagulation. This complements our previous treatment of external mixtures by the QMOM in which four different types of aerosol were simultaneously present (Wright et al., 2000). A rigorous treatment of generally-mixed aerosol populations requires a multivariate description (see Sec. 6) and is reserved for a future report.

2. Derivation of the coupled moment equations for an internal mixture

Consider a general aerosol coordinate x, which can represent particle radius, mass, log radius, etc. The growth law, defined in terms of x, is $\phi(x) \equiv dx/dt$, which in general will depend on condensable vapor species concentrations and temperature, as well as on x. (With closure under arbitrary growth laws enabled by the QMOM, comes the freedom to select the aerosol coordinate that is best for the problem at hand. As explained further in the following sections, this is a very positive feature of the quadrature closure method.) Changes in the aerosol number density distribution function $f(x)$ under condensation and evaporation, which conserve particle number, follow the conservation equation:

$$\frac{\partial f(x)}{\partial t} = -\frac{\partial(\phi f)}{\partial x} \tag{2.1}$$

Units of $f(x)$ are particles per unit volume between x and $x + dx$. The kth moment in x-space is defined as:

$$\left\langle x^k \right\rangle_f \equiv \int_0^\infty x^k f(x)dx \tag{2.2}$$

where $\langle\ \rangle_f$ indicates averaging over the distribution f. Its time evolution is

$$\frac{d}{dt}\left\langle x^k \right\rangle_f = -\int_0^\infty x^k \frac{\partial(\phi f)}{\partial x}dx = k\int_0^\infty x^{k-1}\phi(x) f(x)dx. \tag{2.3}$$

for $k \geq 1$. The first equality follows from Eqs. 2.1 and 2.2. The last equality follows integration by parts and the fact that $f(x)$ vanishes at the limits of integration. The appearance of the total derivative reflects the fact that the integral over size space is a function only of time. For x equal to the particle radius, Eq. 2.3 was derived previously by a similar method (Hulburt and Katz, 1964) and utilized in development of the quadrature method of moments for condensation growth (McGraw, 1997). See the Appendix for a more general result.

Total mass and component species mass distributions

For the remainder of this section let the aerosol coordinate be the total particle mass ($x = m$) and consider the aerosol total mass distribution $q = mf$. Units of $q(m)$ are total aerosol mass per unit volume for those particles having mass between m and $m + dm$. Following Pilinis (1990) and Meng et al. (1998) we define the mass distribution function of species j in the particulate phase:

$$q_j(m,t) = \frac{m_j}{m} q(m,t) \tag{2.4}$$

where $m_j(m)$ is the mass of species j in an internally-mixed particle of total mass m.

To obtain evolution equations for the moments of $q(m)$ and $q_j(m)$ we need the analogous equations to Eq. 2.1 for these distributions. An elegant procedure, based on the

method of characteristics and transformation to the moving reference frame defined by the characteristic curves $dm/dt = \phi(m)$, where $\phi(m)$ is the growth law, has been developed by Pilinis (1990) that solves this problem. Here we give only the final result, referring the reader to Pilinis (1990) and Meng et al. (1998) for additional details of the derivation. For the total mass distribution the analog to Eq. 2.1 is:

$$\frac{\partial q}{\partial t} = -m\frac{\partial(q\phi/m)}{\partial m} = -m\frac{\partial(qH)}{\partial m} \tag{2.5}$$

where the last equality introduces the relative growth law $H(m) = m^{-1}dm/dt$. For the mass distribution of species j the analogous equation is:

$$\frac{\partial}{\partial t}q_j = -\frac{\partial(q_j mH)}{\partial m} + \frac{q}{m}\frac{dm_j}{dt} = -\frac{\partial(q_j mH)}{\partial m} + qH_j(m) \tag{2.6}$$

where the second equality with $H_j(m) \equiv m^{-1}dm_j/dt$ defines the growth law for the relative rate of growth of component m_j in a particle of total mass m. Equation 2.6 is the condensation part of the aerosol general dynamic equation describing evolution of the mass distribution of species j in an internal mixture (Meng et al., 1998).

Evolution of the moments

The mass moments over q are:

$$\left\langle m^k \right\rangle_q \equiv \int_0^\infty m^k q(m)dm \tag{2.8}$$

From this result and $q = mf$ we have the identity:

$$\left\langle m^k \right\rangle_q = \left\langle m^{k+1} \right\rangle_f . \tag{2.9}$$

Thus the zeroth moment over the q-distribution gives the total aerosol mass density. From Eqs. 2.5 and 2.8 and after an integration by parts we obtain:

$$\frac{d}{dt}\left\langle m^k \right\rangle_q = (k+1)\int_0^\infty m^k H(m) q(m) dm . \tag{2.10}$$

for $k \geq 0$. We define the mass moments over q_j as:

$$\left\langle m^k \right\rangle_{q_j} \equiv \int_0^\infty m^k q_j(m) dm . \tag{2.11}$$

Differentiation of Eq. 2.11, using Eq. 2.6 and integrating the first term by parts, gives

$$\frac{d}{dt}\left\langle m^k \right\rangle_{q_j} = k\int_0^\infty m^k q_j(m) H(m) dm + \int_0^\infty m^k q(m) H_j(m) dm \tag{2.12}$$

for $k \geq 0$. (See the Appendix for an alternate derivation of this result.) Equations 2.12 (including one set of moments for each aerosol component j) are the fundamental coupled moment equations of the condensation model. Equation 2.10 for evolution of the aerosol total mass distribution moments is recovered from Eqs. 2.12 by summing over all aerosol components j (using $q = \sum q_j$ and $H = \sum H_j$). Species mass distributions are seen from Eqs. 2.12 to be coupled with each other through the total mass distribution. Equations 2.12 cannot be solved in their present form because of the integrations over the unknown distribution functions $q(m)$ and $q_j(m)$. Except for very special cases of the growth law, closure of these equations is not possible. Specifically, closure of Eq. 2.12 by the conventional method of moments (e.g. Hulburt and Katz, 1964) would require that each of the growth laws, $H(m)$ and $H_j(m)$, be in the form $a + b/m$ where a and b are constants. Analytic solutions for $q(m,t)$, considered by Pilinis (1990) for the growth law $H(m) = a$,

are briefly discussed in Sec. 5. In the following section we outline the closure of Eqs. 2.12 by the quadrature method of moments and introduce a new computational approach (the Jacobian matrix transformation) for their solution.

3. Closure by the quadrature method of moments (QMOM)

A general procedure for closure of moment evolution equations is given by the quadrature method of moments (McGraw, 1997). Indeed all dynamical processes that involve integrations over the unknown aerosol distribution can be handled by this approach. Specifically, the QMOM provides a recipe for closure under coagulation (Barrett and Webb, 1998) as well as for condensation/evaporation growth.

The essence of quadrature based closure of Eqs. 2.10 or 2.12 lies in approximating the growth law integrals by n-point Gaussian quadratures with the non-standard weight function q or q_j. Application of quadrature to Eq. 2.10 gives:

$$\frac{d}{dt}\left\langle m^k \right\rangle_q \cong (k+1)\sum_{i=1}^{n} m_i^k H(m_i) w_i \qquad (3.1a)$$

for $k \geq 0$. The approximate equality in Eq. 3.1a refers to use of the quadrature approximation. The right hand side derives from Eq. 2.10 by treating the unknown distribution $q(m)$ as the weight function, and the known function, $m^k H(m)$, as the kernel. Thus for $q = e^{-m}$ in Eq. 2.10, the rhs of Eq. 3.1a results in the standard n-point Laguerre integration formula whose weights w_i and abscissas m_i are available in tabulated form (Abramowitz and Stegun, 1972). The structure of the rhs of Eq. 3.1a remains valid for non-standard weight functions; only the abscissas and weights need to be determined (see below).

A similar application of the quadrature approximation to each of the terms on the right hand side of Eq. 2.12 gives:

$$\frac{d}{dt}\left\langle m^k \right\rangle_{q_j} \cong k\sum_{i=1}^{n} m_{j,i}{}^{k} H(m_{j,i}) w_{j,i} + \sum_{i=1}^{n} m_i{}^{k} H_j(m_i) w_i \qquad (3.1b)$$

where the subscript i labels the quadrature abscissas m and weights w (for i from 1 to n) and subscript j labels the aerosol component. These are generally different sets for each distribution, which depend only on the lower-order moments of that distribution. The moments themselves are readily expressed in terms of the abscissas and weights. For n-point quadrature:

$$\left\langle m^k \right\rangle_q = \sum_{i=1}^{n} m_i{}^{k} w_i \qquad (3.2a)$$

$$\left\langle m^k \right\rangle_{q_j} = \sum_{i=1}^{n} m_{j,i}{}^{k} w_{j,i} \qquad (3.2b)$$

which are exact for $k = 0$ through $2n-1$.

Mathematical foundation for the QMOM lies in the fact that the abscissas and weights appearing in the quadrature summations for moment evolution (Eqs. 3.1) can be obtained even thought the weight functions $q(m,t)$ and $q_j(m,t)$ are themselves unknown. All that is required is the availability of the lower-order moments of the weight functions (Press and Teukolsky, 1990). This remarkable feature underlies the synergy between quadrature methods, which permit integration of an arbitrary (but known) kernel function over an unknown aerosol distribution (the weight function), and moment methods, which track the lower-order moments of the distribution. Equations 3.2 show that the abscissas and weights are determined by the lower-order moments and this fact leads to closure of Eqs. 3.1. Computing the moments in terms of the abscissas and weights using Eqs. 3.2 is straightforward. A more challenging problem is to invert the first $2n$ moments for $k = 0$ through $2n-1$ to obtain the unique set of n abscissas and n weights for which Eqs. 3.2 are satisfied. One such algorithm is provided by McGraw (1997). Presently we use the compact and efficient subroutine ORTHOG from Numerical Recipes (Press et al., 1992) to

do the inversion. Six-moments, or three-point quadrature points, are often sufficient for estimating aerosol physical and optical properties (McGraw, 1997; McGraw et al., 1995; Yue et al., 1997; Wright, 2000). Accordingly, in the examples given below, we will track six moments, corresponding to three-point quadrature, for each distribution. Tracking the aerosol total mass distribution moments requires using only the six moments of the q-distribution from Eq. 2.8. Tracking the total mass and any one selected component will require 12 moment equations. Tracking all components of a six-component, internally-mixed, aerosol would require 36 moment equations coupled in groupings of six through the total mass distribution, etc.

Inspection of Eqs. 3.1 shows that the differential expressions for moment evolution are given in terms of quadrature abscissas and weights. Except in the special analytic cases mentioned above, for which an exact closed set of equations for moment evolution results, the most direct integration approach requires moment inversion to obtain quadrature abscissas and weights from which moment differentials can be computed via Eqs. 3.1, using these to update the moments, and so on. Thus in this scheme multiple moment inversions are required. Nevertheless this remains a valid and often useful computational approach. Here we will introduce a powerful new method, based on Jacobian matrix transformation (JMT), for obtaining closure in the QMOM while preserving the rigorous correspondence between the moments and the quadrature abscissas and weights. The JMT closure has significant advantages for describing continuous evolution of an aerosol population in time. Specifically, the JMT eliminates the need for repeated moment inversions. As most aerosol dynamic processes, including condensation, chemistry, coagulation, and removal are continuous, the method is quite general and not limited to the particular moment evolution described by Eqs. 3.1. An important exception to continuous aerosol dynamics is the transport step in an Eulerian model, which necessarily involves transfer of finite amounts of all species, including moments, from cell to cell at each transport time step. Another example is primary emissions, which can introduce finite changes in aerosol moments over a model time step. At these junctures, which involve finite changes in the moments during a

model run, a moment inversion step [for example using (McGraw, 1997) or ORTHOG] to update the quadrature abscissas and weights is required. Between such steps, during which continuous evolution of the aerosol occurs, the JMT can be used. Besides making closure more explicit, the JMT is a powerful analytic tool that can often be used to simplify propagation of the abscissas and weights. These features are illustrated below.

Jacobian matrix transformation (JMT):

The JMT enables a closed set of differential equations to be obtained solely in terms of the abscissas and weights. To illustrate the method, return to the general coordinate notation of Eqs. 2.1-3 and consider a generic set of moments $\vec{\mu} = \{\mu_0, \mu_1, ..., \mu_{2n-1}\}$ and corresponding abscissas $\{x_i\}$ and weights $\{w_i\}$ represented by the vector $\vec{r} = \{x_1, w_1, x_2, w_2, ..., x_n, w_n\}$. The latter are connected with the moments through Eqs. 3.2c:

$$\mu_k \equiv \int x^k f(x) dx = \sum_{i=1}^{n} x_i^k w_i \tag{3.2c}$$

From Eqs. 3.2c we obtain the Jacobian matrix $\mathbf{J}$ defined as:

$$\mathbf{J} \equiv \begin{pmatrix} \frac{\partial \mu_0}{\partial x_1} & \frac{\partial \mu_0}{\partial w_1} & \cdots & \frac{\partial \mu_0}{\partial w_n} \\ \frac{\partial \mu_1}{\partial x_1} & \frac{\partial \mu_1}{\partial w_1} & \cdots & \frac{\partial \mu_1}{\partial w_n} \\ & & \vdots & \\ \frac{\partial \mu_{2n-1}}{\partial x_1} & \frac{\partial \mu_{2n-1}}{\partial w_1} & \cdots & \frac{\partial \mu_{2n-1}}{\partial w_n} \end{pmatrix} = \begin{pmatrix} 0 & 1 & \cdots & 1 \\ w_1 & x_1 & \cdots & x_n \\ & & \vdots & \\ (2n-1)x_1^{2n-2} w_1 & \cdots & & x_n^{2n-1} \end{pmatrix} \tag{3.3}$$

The elements of $\mathbf{J}$, shown in the last array, are easily obtained from Eqs. 3.2c and involve only the abscissas and weights. Multiplication by the above matrix yields the differentials for the moments in terms of differentials for the abscissas and weights: $d\vec{\mu} = \mathbf{J} d\vec{r}$. This is a linear system that is readily solved numerically for $d\vec{r}$.

Explicit solution for $d\vec{r}$ requires the Jacobian matrix of the inverse transformation $\mathbf{J}^{-1}$ whose derivatives are reciprocal to those of Eq. 3.3. Multiplication of the vector of moment differentials $d\vec{\mu} = \{d\mu_0, d\mu_1, ..., d\mu_{2n-1}\}$ by $\mathbf{J}^{-1}$ yields the vector of differentials for the abscissas and weights $d\vec{r} = \{dx_1, dw_1, dx_2, dw_2, ..., dx_n, dw_n\}$:

$$d\vec{r} = \mathbf{J}^{-1} d\vec{\mu} \ . \tag{3.4}$$

Given that the elements of both factors on the right hand side of Eq. 3.4, $d\vec{\mu}$ from Eqs. 3.1 and $\mathbf{J}^{-1}$, involve only abscissas and weights, Eq. 3.4 is a closed set of differential equations in these quantities. Initial values for the abscissas and weights are obtained from the initial moments on inversion. To carry out this procedure in general, the quadrature approximation, indicated by the approximate equality for $d\vec{\mu}$ in Eqs. 3.1a and 3.1b is required. However for those special cases that an exact closed-form set of equations can be obtained for the moments it follows, because the moments are related to the abscissas and weights through Eq. 3.2c, that Eq. 3.4 is also exact. This is demonstrated for analytic test cases in Sec. 5. Like the QMOM itself, the JMT provides a more general framework for representing aerosol dynamics than does the conventional method of moments, reducing to the latter whenever the latter is exact.

For analytic results, as in the derivation of Eqs. 3.5 below, explicit expressions for the elements of $\mathbf{J}^{-1}$ may be needed. These are significantly more complicated than those of $\mathbf{J}$ but are readily evaluated using a symbolic computation program such as Mathematica (Wolfram, 1999). These elements are universal for 3-point quadrature as they depend only on the mathematical transformation between abscissas and weights and moments and not on the functional form of $d\vec{\mu}$. Thus the same matrices, $\mathbf{J}$ and $\mathbf{J}^{-1}$, apply to any aerosol process including, for example, the representation of multicomponent coagulating aerosols (Sec. 4). Note that if a pair of abscissas were to coincide, or a weight vanish, the matrix of

Eq. 3.3 would be singular and $\mathbf{J}^{-1}$ would not be defined. In practice this case doesn't arise, but the issue can be forced by requiring that the distribution consist of only one or two delta functions. Even in these very unnatural cases, nonsingularity is easily restored by taking into account the true lower dimensionality of $\mathbf{J}$ and $\mathbf{J}^{-1}$. Closure equations for the q and q_j distributions are now given for 3-point quadrature.

Closure equations for the total aerosol mass distribution $q(m)$:

Substitution of Eq. 3.1a into Eq. 3.4 and taking the time derivative of both sides yields an especially simple result for evolution of the abscissas and weights under condensation growth:

$$\frac{d}{dt}\begin{pmatrix} m_1 \\ w_1 \\ \vdots \\ m_3 \\ w_3 \end{pmatrix} = \mathbf{J}^{-1}\{m_i;w_i\}\begin{pmatrix} H(m_1)w_1 + \ldots + H(m_3)w_3 \\ 2m_1H(m_1)w_1 + \ldots + 2m_3H(m_3)w_3 \\ \vdots \\ 5{m_1}^4H(m_1)w_1 + \ldots + 5{m_3}^4H(m_3)w_3 \\ 6{m_1}^5H(m_1)w_1 + \ldots + 6{m_3}^5H(m_3)w_3 \end{pmatrix} = \begin{pmatrix} m_1H(m_1) \\ w_1H(m_1) \\ \vdots \\ m_3H(m_3) \\ w_3H(m_3) \end{pmatrix} \qquad (3.5a)$$

where the elements of $\mathbf{J}^{-1}$ are the same as above, but here in terms of the abscissas and weights $\{m_i;w_i\}$ of the q distribution. Although the middle expression is quite complicated it reduces, aided by the algebraic capabilities of Mathematica, to the extremely simple result shown on the right. Equations 3.5a are the natural evolution equations for a decoupled set of monodisperse distributions of particles of mass m_i and can be rewritten as:

$$\begin{aligned} \frac{dm_i}{dt} &= m_iH(m_i) \\ \frac{dw_i}{dt} &= w_iH(m_i) \end{aligned} \qquad . \qquad (3.5b)$$

For continuous evolution of single-component aerosols under condensation and evaporation, Eqs. 3.5b can be used directly and there is no need for moment inversion to

update the abscissas and weights. It can be shown that the first of Eqs. 3.5b, giving rise to a pure evolution of the abscissas (dm_i / dt), results from the leading term, proportional to k on expansion of the right hand side of Eq. 3.1a. The second of Eqs. 3.5b, giving rise to a pure propagation of the weights (dw_i / dt), results from the remaining term proportional to unity.

Closure equations for the aerosol component mass distribution $q_j(m)$:

Evolution of the abscissas and weights for the j-component distributions from Eqs. 3.1b and 3.2b is slightly more complicated. One reason is that without knowledge of the q-distribution at the quadrature points of the q_j-distribution, and vice versa, it is generally not possible to approximate both integrals in Eq. 2.12 using the same set of abscissas and still have *exact representation of the lower-order moments of each distribution.* For this we must utilize all $2n$ quadrature points (n for the component j distribution and n for the total mass distribution) that appear on the right hand side of Eqs. 3.1b. Nevertheless, evolution of the abscissas and weights of the q_j-distribution can still be carried out rigorously by the Jacobian matrix transformation method. (Of course if the composition m_j / m in Eq. 2.11 is independent of m, the distributions are proportional and the problem simplifies considerably. Here we will examine the more general case.)

We begin by splitting the moment time derivative into two parts according to $d\vec{\mu} / dt = d_1\vec{\mu} / dt + d_2\vec{\mu} / dt$ where $d_1\vec{\mu} / dt$ and $d_2\vec{\mu} / dt$ are, respectively, the first and second terms on the right hand side of Eq. 3.1b. These give rise to the corresponding increments $d_1\vec{r} / dt$ and $d_2\vec{r} / dt$ in the abscissas and weights. The first term, which contains abscissas and weights from only the q_j-distribution is most easy to evaluate and reduces to a simple evolution of the abscissas with no change in the weights:

$$\frac{d_1}{dt}\begin{pmatrix} m_{j,1} \\ w_{j,1} \\ m_{j,2} \\ w_{j,2} \\ m_{j,3} \\ w_{j,3} \end{pmatrix} = \mathbf{J}^{-1}\{m_{j,i};w_{j,i}\}\frac{d_1}{dt}\vec{\mu} = \begin{pmatrix} m_{j,1}H(m_{j,1}) \\ 0 \\ m_{j,2}H(m_{j,2}) \\ 0 \\ m_{j,3}H(m_{j,3}) \\ 0 \end{pmatrix}. \qquad (3.6a)$$

The elements of $\mathbf{J}^{-1}$ have the same functional form as previously, but are now in terms of the abscissas $m_{j,i}$ and weights $w_{j,i}$ of the q_j distribution. The contribution from the $d_2\vec{r}/dt$ involves abscissas and weights from both the q and q_j distributions and is a more complicated expression:

$$\frac{d_2}{dt}\begin{pmatrix} m_{j,1} \\ w_{j,1} \\ m_{j,2} \\ w_{j,2} \\ m_{j,3} \\ w_{j,3} \end{pmatrix} = \mathbf{J}^{-1}\{m_{j,i};w_{j,i}\}\begin{pmatrix} H_j(m_1)w_1 + \ldots + H_j(m_3)w_3 \\ m_1H_j(m_1)w_1 + \ldots + m_3H_j(m_3)w_3 \\ \vdots \\ m_1{}^4H_j(m_1)w_1 + \ldots + m_3{}^4H_j(m_3)w_3 \\ m_1{}^5H_j(m_1)w_1 + \ldots + m_3{}^5H_j(m_3)w_3 \end{pmatrix}. \qquad (3.6b)$$

Although we have not found a simpler result for the right hand side of Eq. 3.6b, the latter is readily evaluated given $\mathbf{J}^{-1}$. The vector on the right hand side of Eq. 3.6b contains the abscissas and weights of the q distribution and the matrix-vector product, therefore, contains contributions from both distributions as expected. The total differential change for the abscissas and weights of the component distribution is obtained by summing Eqs. 3.6a and 3.6b. The result, together with the equation for evolving the abscissas and weights of the q distribution (Eq. 3.5), constitute a closed set of 12 equations for evolution of the abscissas and weights of both (total mass and component j) distributions. Sets of

equations identical to Eqs. 3.6 are encountered for each of the aerosol component distributions. Although more complicated than using a single set of abscissas, this procedure insures optimal representation of the moments for each distribution.

4. Coagulation by the QMOM

Coagulation rates are frequently expressed in terms of particle volume, however in this section we will continue the notation of Secs. 2 and 3 and express distributions in terms of particle mass. Conversion to volume or radial moments is straightforward for spherical particles of known density. Evolution of the kth moment under coagulation can be written as (Barrett and Webb, 1998):

$$\left(\frac{d}{dt}\left\langle m^k\right\rangle_f\right)_{coag} = \frac{1}{2}\int_0^\infty du\int_0^\infty dv\left[(u+v)^k - u^k - v^k\right]K(u,v)\,f(u,t)\,f(v,t) \qquad (4.1)$$
$$\cong \frac{1}{2}\sum_{i=1}^{n}\sum_{j=1}^{n}\left[(m_{f,i}+m_{f,j})^k - m_{f,i}{}^k - m_{f,j}{}^k\right]K(m_{f,i},m_{f,j})w_{f,i}w_{f,j}$$

where the coordinates u and v refer to particle mass and the subscript f labels the abscissas and weights of the f-distribution. The integrand in Eq. 4.1 derives form considering the coagulation of a pair of particles of masses u and v to form a particle of total mass $u+v$ and the effect that each such event has on the moment. $K(u,v)$ is the collision frequency function, which depends on the volumes of the colliding particles and on such properties of the system as temperature, pressure, and viscosity. The factor of 1/2 corrects for double counting. The last equality gives the approximate moment evolution in the QMOM. As with condensation, closure is obtained from the connection between moments and quadrature abscissas and weights.

This result will now be extended to the case of coagulation for an internally-mixed multicomponent aerosol to obtain the moment evolution for the $q(m)$ and $q_j(m)$ distributions. A similar result to Eq. 4.1 is readily obtained for evolution of the moments of the aerosol total mass distribution, $q(m)$. From Eqs. 2.9 and 4.1 we obtain:

$$\left(\frac{d}{dt}\left\langle m^k\right\rangle_q\right)_{coag} = \frac{1}{2}\int_0^\infty du\int_0^\infty dv\left[(u+v)^{k+1} - u^{k+1} - v^{k+1}\right](uv)^{-1}K(u,v)q(u,t)q(v,t)$$
$$\cong \frac{1}{2}\sum_{i=1}^{n}\sum_{j=1}^{n}\left[(m_i+m_j)^{k+1} - m_i^{k+1} - m_j^{k+1}\right](m_i m_j)^{-1}K(m_i,m_j)w_i w_j \qquad (4.2a)$$

where the double summations are over the abscissas and weights for the $q(m)$ distribution. The evolution of $q_j(m)$ due to coagulation is given by Pilinis (1990):

$$\frac{\partial q_j(m,t)}{\partial t} = \frac{1}{2}\int_0^m K(m', m-m')q_j(m',t)\frac{q(m-m',t)}{m-m'}dm'$$
$$- q_j(m,t)\int_0^\infty K(m,m')\frac{q(m',t)}{m'}dm'$$

The first term on the right hand side describes the production of particles of mass *m* through coagulation of particles of masses m' and $m-m'$, and the second term describes the loss of particles of mass *m* as these coagulate with particles of mass m'. Using this result to differentiate the integrand of Eq. 2.11 and carrying out the integration, we obtain the following rate of change for the kth moment:

$$\left(\frac{d}{dt}\left\langle m^k\right\rangle_{q_j}\right)_{coag} = \frac{1}{2}\int_0^\infty du\int_0^\infty dv\left[(u+v)^k - u^k\right]v^{-1}K(u,v)q_j(u,t)q(v,t)$$
$$+\frac{1}{2}\int_0^\infty du\int_0^\infty dv\left[(u+v)^k - v^k\right]u^{-1}K(u,v)q_j(v,t)q(u,t)$$
$$\cong \sum_{i=1}^{n}\sum_{l=1}^{n}\left[(m_{j,i}+m_l)^k - m_{j,i}^{\ k}\right](m_l)^{-1}K(m_{j,i},m_l)w_{j,i}w_l \qquad (4.2b)$$

where i and l are summation indices and j, as in Eqs. 3.2, labels the aerosol component. In the first integral $u = m'$ and $v = m - m'$; in the second $u = m'$ and $v = m$. The last equality follows from the permutation symmetry $K(u,v) = K(v,u)$. As in Eq. 3.1b, the abscissas and weights for both distributions, $q(m)$ and $q_j(m)$, appear on the right hand side

of Eq. 4.2b. Summation of the equalities of Eq. 4.2b for different species index j gives Eq. 4.2a.

Equations 4.2 complete the QMOM formulation for moment evolution under coagulation of internal mixtures described by the $q(m)$ and $q_j(m)$ distributions. Together with Eqs. 3.2 for the moments, a closed set of equations for the lower-order moments is obtained as in the case of condensation. Closure equations, which do not require multiple moment inversions to update the abscissas and weights, can be also be obtained for coagulation using the Jacobian matrix transformation of Sec. 3. In the notation of Eq. 3.4, with subscript labels added to indicate the distribution, we obtain

$$\left(\frac{d\vec{r}_q}{dt}\right)_{coag} = \mathbf{J}^{-1}\{m_i; w_i\}\left(\frac{d\vec{\mu}_q}{dt}\right)_{coag} \tag{4.3a}$$

$$\left(\frac{d\vec{r}_{q_j}}{dt}\right)_{coag} = \mathbf{J}^{-1}\{m_{j,i}; w_{j,i}\}\left(\frac{d\vec{\mu}_{q_j}}{dt}\right)_{coag} . \tag{4.3b}$$

where the kth elements of the moment vector derivatives are given by Eqs. 4.2. (Note the abbreviated notation whereby the kth component of $\vec{\mu}_q$ equals $\langle m^k \rangle_q$, etc.) The $\mathbf{J}^{-1}$ matrices of Eqs. 4.3a and 4.3b are identical to those of Eq. 3.5a and Eq. 3.6, respectively. A similar equation to Eq. 4.3a results for evolution of the abscissas and weights and moments of the f distribution. In this case $\mathbf{J}^{-1}$ has the same functional form as above, but its arguments are given in terms of the abscissas and weights of the number distribution. Equations 4.3 describe continuous evolution of abscissas and weights under coagulation in much the same way that Eqs. 3.5 and 3.6 do under condensation. The differentials from Eqs. 3.5a and 4.3a for $q(m)$ [from Eqs. 3.6 and 4.3b for $q_j(m)$] contribute additively to the aerosol general dynamic equation describing continuous evolution under simultaneous condensation and coagulation. These results are illustrated in the calculations below.

5. Calculations

Analytic solutions for $q(m,t)$ under conditions of constant coagulation kernel and constant growth rates are given by Pilinis (1990). These conditions, with coagulation and condensation occurring separately or together, result in closed-form equations for moment evolution and both the MOM and the QMOM are exact. In addition to evolution under a constant kernel, the sum and product coagulation kernels, $K(u,v) = u + v$ and $K(u,v) = uv$, are also handled exactly by moment methods for the positive integral moments (Barrett and Webb, 1998). To benchmark the QMOM for a non-analytic case, we use the coagulation kernel for Brownian coagulation in the continuum (large particle) regime (Friedlander and Wang, 1966):

$$K(u,v) = K_{BL}(u^{1/3} + v^{1/3})(u^{-1/3} + v^{-1/3}) \tag{5.1}$$

where u and v are particle volumes. The prefactor K_{BL} depends on temperature and viscosity and will be assumed constant in the calculations to follow.

For growth by condensation, a widely used interpolation formula, which provides a non-analytic test case for the model (Barrett and Clement, 1988; McGraw et al., 1998) is:

$$H(m) = A\frac{m^{-1/3}}{a_M + m^{1/3}}. \tag{5.2}$$

The prefactor, A, is proportional to the difference in number density of condensable molecules in the vapor at large distance from the particle and the number density at the particle surface. This difference is positive for condensation and negative for evaporation. The parameter a_M is dependent on the mass accommodation coefficient and mean free path. Without loss of generality we can express mass in units of $a_M{}^3$, and time in units of $a_M{}^2 / A$, to obtain:

$$\tilde{H}(\tilde{m}) = \frac{\tilde{m}^{-1/3}}{1+\tilde{m}^{1/3}} \tag{5.3}$$

where the tilde indicates reduced units ($\tilde{m} = m/a_M{}^3$; $\tilde{t}_{cond} = At/a_M{}^2$). For coagulation it is conventional to express results in terms of the reduce time $\tilde{t}_{coag} = K_{BL}N_0 t$ where N_0 is the initial particle number density, and reduced particle number N/N_0.

For the general case that both condensation and coagulation are occurring, because only one reduced time scale can be chosen, we express time in terms of $\tilde{t}_{cond}$ using the time constant ratio $\chi = a_M{}^2 K_{BL} N_0 / A$ to determine the relative rates of the two processes. Thus for $\chi << 1$ condensation occurs more quickly than coagulation, and vice versa. In the simultaneous process calculations below we choose $\chi = 1$.

Benchmark box-model calculations: Discrete scheme for solving the aerosol general dynamic equation

To evaluate the QMOM for multicomponent aerosols we computed benchmark results using a discrete representation of the particle size distribution. The discrete scheme employed here numerically integrates the appropriate terms of the aerosol general dynamic equation for growth by coagulation and condensation using a fixed logarithmic mass scale. The scheme is optimized for ease of programming and is not designed to minimize the number of grid points or computation speed. In practice the number of grid points is increased until convergence is obtained. As evolution processes give rise to particle masses that do not correspond to any of the fixed grid values, these are apportioned over the neighboring grid points.

As an illustration suppose that there are N coagulation events between particles of masses m_i and m_j (grid points i and j) during an integration time step. This would yield N particles of mass $m_k = m_i + m_j$, with $m_{nlo} \le m_k < m_{nhi}$ where m_{nlo} and m_{nhi} are the masses of the two neighboring grid points nlo and nhi, respectively. The mass contained

in the N particles of mass m_k is apportioned between grid points *nlo* and *nhi* such that the number of new particles N and the total mass Nm_k are both conserved during the apportionment. This is done by solving the pair of equations $N = N_{nlo} + N_{nhi}$ and $Nm_k = N_{nlo}m_{nlo} + N_{nhi}m_{nhi}$ for N_{nlo} and N_{nhi}, the increments added to the numbers of particles at grid points *nlo* and *nhi*, respectively. For an initial distribution with size-independent composition, coagulation alone does not change particle composition and the moments of each component are simply related to the moments of the total mass distribution. For the general case where particle composition is size-dependent, the mass per particle for each component must be updated by considering at each coagulation event the mass of each component acquired by the relevant grid points, as well as the changes in particle number for those points. Comparison with the finite-element method (FEM) results of Barrett and Webb (1998) shows good agreement taking into account the degree of convergence of the FEM results suggested by their tabulated values.

During condensation, each of the N_i particles of mass m_i acquires mass dm_i during the time step with $m_i \le m_i + dm_i < m_{i+1}$. The time step is kept small enough to insure that the latter inequality is satisfied. As in the treatment of coagulation described above, the total mass contained in the N_i particles of mass $m_i + dm_i$ is apportioned between neighboring grid points i and $i+1$ such that total mass and number are conserved. The composition of each grid point is updated by computing the mass of each component that condenses on a particle of total mass m_i during a time step for each of the grid points. For growth by simultaneous coagulation and condensation, operator splitting is used. The mass range of the grid is extended far enough to insure that the distribution amplitude is negligible at the high-mass end of the spectrum.

Variable transformation in the QMOM

For developing the evolution equations for the abscissas and weights in Secs. 3 and 4 it was convenient to work in terms of the first six positive integral mass moments $q(m)$:

m^k for $k = 0$ through 5. In the calculations presented below we use the fractional moments ($\left\langle m^{k/3} \right\rangle$ for $k = 0$ through 5). For an aerosol of uniform particle density these mass-fractional moments are proportional to the radial moments. This choice is motivated by the fact that the members of this fractional moment sequence are of greater physical relevance than higher-order members of the corresponding integral moment sequence (Tandon and Rosner, 1999). Furthermore, attempts to accurately represent the higher integral moments, for example the fifth mass moment of $q(m)$, magnify the importance of the tail of the distribution, which is heavily weighted, and greatly increases the difficulty of carrying out numerical calculations with sufficient accuracy and resolution to provide a good benchmark test for the QMOM.

A very useful feature of the QMOM is that coordinate transformations can be implemented simply by modifying the initial abscissas and weights and then evolving these in time using the same transformations (e.g. the same Jacobian and the same $d\vec{\mu}$) as used in evolution of the integral moments. This is seen for the fractional $k/3$ mass moments as follows. Let the JMT evolution of the abscissas and weights, as determined initially from the $t = 0$ integral moments, be represented schematically as follows:

$$\left\{ m_i(0), w_i(0) \right\} \underset{JMT}{\rightarrow} \left\{ m_i(t), w_i(t) \right\} \tag{5.4}$$

Next consider transformation to fractional $k/3$ mass moments and let $\eta = m^{1/3}$. The fractional mass moments are:

$$\left\langle m^{k/3} \right\rangle_q \equiv \int_0^\infty m^{k/3} q(m) dm = \int_0^\infty \eta^k q_\eta(\eta) d\eta \cong \sum_{i=1}^n \eta_i^k w_i \tag{5.5}$$

where the middle equality uses the transformation rule, $q_\eta(\eta)d\eta = q(m)dm$, underlying the mapping between coordinate systems. The fractional moment sequence $\left\langle m^{k/3} \right\rangle$ at $t = 0$ (e.g. for $k = 0$ through 5), when processed through ORTHOG, yields the corresponding

initial set of abscissas and weights $\{\eta_i(0), w_i(0)\}$. One can now evolve $\{\eta_i, w_i\}$ using the same JMT as previously used to evolve the integral moments. This requires first cubing the abscissas to obtain units of mass and then evolving the cubed abscissas and weights as in Eq. 5.4:

$$\left\{ \eta_i^3(0), w_i(0) \right\} \underset{JMT}{\rightarrow} \left\{ \eta_i^3(t), w_i(t) \right\}. \tag{5.6}$$

The fractional mass moments at time t are obtained from the right hand side of Eq. 5.6:

$$\left\langle m^{k/3} \right\rangle_q \cong \sum_{i=1}^{n} (\eta_i^3)^{k/3} w_i \tag{5.7}$$

Other variable transformations are readily accommodated by this approach using similar transformations for the abscissas and weights.

Comparison between the benchmark model calculations and the QMOM

The initial number distribution is taken to be log-normal in the calculations that follow:

$$f(m,0) = N_0 \left(ms\sqrt{2\pi} \right)^{-1} \exp\{-[\ln(m/\overline{m})]^2 / (2s^2)\}. \tag{5.8}$$

N_0 is the particle number density, m is particle mass, $\overline{m}$ is the geometric mean mass, and s is the logarithm of the geometric standard deviation. [The m in Eq. 5.8 is the mass in reduced units, $\tilde{m}$, (c.f. Eq. 5.3) however to avoid a separate notation we simply set $a_M = 1$ and $m = \tilde{m}$.] The initial mass moments of $q(m,0) = mf(m,0)$ are:

$$\mu_k(0) = \exp\{(k+1)\overline{m} + [(k+1)s]^2 / 2\} \tag{5.9}$$

after normalization by the initial particle number, N_0. In the calculations that follow we set $s^2 = Log(4/3)$, and $\overline{m} = \sqrt{3}/2$. For the species distributions we set $q_j(m,0) = q(m,0)/3$ for $j = a,b,c$ and for the individual species growth laws,

$\tilde{H}_a(m) = 0$, $\tilde{H}_b(m) = \tilde{H}(m)/3$, and $\tilde{H}_c(m) = 2\tilde{H}(m)/3$. The tilde signifies reduced time units. Finally we assume unit densities and report results in terms of particle volume, v.

Figure 1, shows convergence of the benchmark model calculations for the full distribution function and for the largest fractional moment ($\mu_{5/3}$) under continuum Brownian coagulation alone. The lower panel gives percent error, as compared with the QMOM, vs reduced time [$\%e = 100(QMOM - Grid)/Grid$] where 'QMOM' and 'Grid' are the moments from the QMOM and numerical calculations respectively. We note that the errors always decrease as the number of grid points increases. Because the QMOM result is fixed, this is a measure of the convergence of the discrete grid results. These results show that high grid resolution is necessary for accurate benchmarking of the moment calculations (especially for the higher-order moments). This is a reflection of the high accuracy of the QMOM, which requires even higher accuracy of any benchmark calculation. The distribution function itself appears well converged using just 100 grid points, while the error in the highest moment, $\mu_{5/3}$, which differs most from the converged result, is about 1%. Note the logarithmic scale, used in the upper panel, shows significant evolution of $f(v)$ form the initial distribution to the distribution at reduced time $\tilde{t} = 10$, suggesting a reasonable test case for the QMOM. Coordinates have been chosen so as to preserve area under the conservation of total particle volume that takes place during coagulation alone.

Figure 2 shows moment evolution under simultaneous condensation and coagulation (for $\chi = 1$) from the discrete representation (3000 grid points) and from the QMOM (dots). The QMOM results were obtained without operator splitting (dots) and show much larger departure from the discrete calculations than was found for either of the processes, coagulation and condensation, separately. This discrepancy is attributed to degradation by operator splitting of the accuracy of the discrete calculations. To access the influence of operator splitting, calculations were carried out for $q(v)$ by modifying the QMOM so as to use the same operator splitting method as in the discrete case. The results

(open diamonds) never exceed a percent error difference of 0.5% from the discrete benchmark calculations. Thus the original QMOM results without operator splitting are probably accurate to within the 0.5% error range expected from our analysis of the coagulation and condensation processes separately.

In addition to benchmarking against computationally intensive simulations using high-resolution grids, there are several analytic cases and cases of known asymptotic behavior that provide additional tests on the accuracy of the QMOM.

Analytic and asymptotic results by the QMOM

For the analytic test cases considered by Pilinis either $H(m) = 1$ or $K(u,v) = 1$, or both (Pilinis, 1990). Under these conditions, moment methods, including the QMOM, are exact for the positive integral mass moments. This property follows from the fact that these simplified growth laws yield closed sets of equations for the integral moments (see previous discussion and Barrett and Webb, 1998). Analytic cases for which the full distributions are known exactly as a function of time provide a good benchmark for the accuracy of the QMOM integration methods described in Sec. 3. Table 1 shows results for evolution of the fractional $1/3$ moments under simultaneous condensation and coagulation (for $H(m) = 1$ and $K(u,v) = 1$) and comparison with analytic moments obtained from the full distribution (since the latter is known analytically, all moments including the integral and the fractional $1/3$ moments are also known). Even with substantial evolution from the initial conditions, excellent agreement is found for both the integral moments (μ_0 and μ_1) and the fractional moments. In the former case agreement is expected and these results demonstrate that errors due to numerical integration are exceedingly small. Excellent agreement for the fractional moments is an indicator of the accuracy that can be expected from 3-point quadrature integration even for problems for which the method is not exact.

The accuracy of the QMOM for long-time evolution under coagulation can be benchmarked by comparison with asymptotic results (Friedlander and Wang, 1966). The asymptotic distribution is the similarity, or self-preserving, form that results for the

continuous distribution function based on the property that the fraction of particles in a given size range is a function only of the dimensionless volume $\eta = v / \bar{v}$ where $\bar{v}$ is the average particle volume. In terms of the volume moments of the number distribution, $f(v)$, $\bar{v} = \mu_1 / \mu_0$. In general both the total particle volume $V = \mu_1$ and number density $N_\infty = \mu_0$ are functions of time. Here we consider the simplest case for which no material is added or lost (constant V) and the number density decreases as coagulation takes place. In this notation the relation:

$$\frac{f(v)dv}{N_\infty} = \psi\left(\frac{v}{\bar{v}}\right)d\left(\frac{v}{\bar{v}}\right) \tag{5.10}$$

defines the reduced distribution function $\psi(\eta)$. At long times, as $\psi(\eta)$ reaches its asymptotic self-preserving form, the moments of $\psi(\eta)$:

$$\omega_k \equiv \int_0^\infty \eta^k \psi(\eta) d\eta \tag{5.11}$$

will also approach asymptotic values. In terms of the moments of $f(v)$, the reduced moments are:

$$\omega_k = \left(\frac{\mu_k}{\mu_0}\right)\left(\frac{\mu_0}{\mu_1}\right)^k. \tag{5.12}$$

To compare our calculations with asymptotic results we evolve the moments, $\mu_k(t)$, of $f(v,t)$ out to long time using the QMOM. From these are determine the nondimensional moments, $\omega_k(t)$ of the reduced distribution using Eq. 5.12. Two different coagulation kernels, the analytic constant kernel and the continuum Brownian kernel were used to evolve the moments. Convergence of the reduced moments to their asymptotic values is shown in Fig. 6 for coagulation via the continuum Brownian kernel. The integration time was taken out to $t = 10^5$ although reliable convergence is obtained in considerably less time (Fig. 6). The logarithmic time scale is used to emphasize the approach to asymptotic behavior. Calculations were performed on a Sun Spark Enterprise

and required only a few seconds of computer time using the Jacobian matrix transformation.

Asymptotic values of the reduced moments (here taken to be the values at $t = 10^5$) are given in Table 2. For the constant kernel, the analytic distributions and thus the moments are known exactly and the ω_k are known to approach the factorial values $\omega_k = \Gamma(k+1)$ (Wang, 1966). The QMOM results are seen to be in excellent agreement with the analytic values as expected in the constant kernel case for which, apart from numerical roundoff, the QMOM is exact. The agreement for α, which is defined in terms of the fractional $1/3$ volume moments (see caption) is good only to about 5%, reflective of the fact that the QMOM is not exact for fractional moments. QMOM results for the continuum Brownian kernel are also shown and seen to be in excellent agreement with literature values for the integral volume moments and for α (exact results are not available for this case).

6. Summary and discussion

Moment methods, and in particular the QMOM, provide a highly accurate tool for tracking the moments of a particle size distribution. In this paper these methods have been extended to internally-mixed particle populations and tested through simulations of particle evolution through condensation and coagulation growth. The percent errors, which were the greatest for the highest order moment, never exceeded 0.05% for coagulation, 0.4% for condensation, and an estimated 0.5% for the combined processes without operator splitting. The accuracy for coagulation is especially remarkable and may be due to constraints on how the moments evolve under the QMOM. For example, unless two colliding particles are very different in size, the Brownian kernel is nearly constant - and moment evolution for a constant kernel by the QMOM is exact (Sec. 5). Self-preserving constraints on the distribution function may also serve to prevent unbounded accumulation of error as the moments of a coagulating aerosol are evolved for long times using the QMOM. The QMOM was found to give exact results for the asymptotic moments in the constant kernel case and excellent agreement with literature values for the asymptotic moments derived from

self-preserving size distributions in the continuum Brownian case. This paper also introduced the Jacobian matrix transformation (JMT) and demonstrated its use as an alternate closure method for the QMOM.

Previous applications of moment methods have generally been limited to univariate distributions in which a single coordinate, usually particle radius or mass, is used to represent particle size. The internal mixture assumption employed in the present study also results in a one-dimensional aerosol representation with total particle mass as coordinate. However, with internal mixtures, multiple distributions, one for each component species, need to be tracked and these are coupled through the total particle mass. The methods described in this paper provide a solution to the representation of internal mixtures in aerosol models by moment methods.

The development of multicomponent thermodynamic models (e.g., Clegg et al., 1998; Capaldo et al., 2000), has enabled improved prediction of aerosol evaporation rates and gas-particle exchange. The resulting growth laws have more general composition dependence than those considered here, e.g., species growth rates of the multivariate form, $H_j(m_1, m_2, ...)$, in the notation of Sec. 2. The great efficiency of moment methods makes these ideal candidates for extension to multivariate problems. An important step in that direction was recently taken through the development of a bivariate extension of the QMOM for modeling simultaneous coagulation and sintering of nonspherical particle populations (Wright et al., 2001). Most recently, a fully multivariate version of the QMOM has been developed using a dynamic extension of principal component analysis to provide the mapping between mixed-moment elements of the multivariate covariance matrix and the quadrature abcissas and weights. Results from these studies will be reported in future work (Yoon and McGraw, 2002).

Appendix: A generalized derivation of Eqs. 2.3 using the Reynold's transport theorem

Consider an integral over the particle number distribution function of the form:

$$I = \iiint h(\vec{x})\, f(\vec{x},t)\, dV \tag{A1}$$

where $f(\vec{x},t)$ is the (here multivariate) distribution function, with $\vec{x} \equiv (x_1, x_2, ..., x_k)$, and $h(\vec{x})$ is a kernel that depends that depends only on $\vec{x}$. Because $f(\vec{x},t)$ is conserved under growth by condensation, and assuming that there are no sinks or sources of particles within the integration volume, it satisfies the continuity equation:

$$\frac{df}{dt} + f(\nabla \cdot \vec{v}) = \frac{\partial f}{\partial t} + \nabla \cdot (f\vec{v}) = 0 \tag{A2}$$

where $\vec{v} = \phi(\vec{x}) = d\vec{x}/dt$ is a generalization of the univariate growth rate, $\phi(x)$, of Sec. 2 to the multivariate case. $\partial / \partial t$ denotes rate of change at constant $\vec{x}$ and d/dt is the rate of change in the frame of the particle, analogous to the "material derivative" (Aris, 1962) used in the case of fluid flow.

Under these conditions, we can adapt the methods described by Aris (1962) to obtain the temporal evolution of A1:

$$\begin{aligned} \frac{dI}{dt} = \frac{d}{dt}\iiint hf dV &= \iiint \left\{ \frac{d}{dt}(hf) + hf(\nabla \cdot \vec{v}) \right\} dV \\ &= \iiint \left\{ f\frac{dh}{dt} + h\left(\frac{df}{dt} + f\nabla \cdot \vec{v} \right) \right\} dV = \iiint f \frac{dh}{dt} dV \end{aligned} \tag{A3}$$

where the second equality is the Reynold's transport theorem (Aris, 1962) and the fourth equality follows from Eq. A2. Note here that the volume of integration is assumed large enough contain all of the particles independent of time. Equation A3 is the more general result mentioned in Sec. 2. It reduces to Eq. 2.3 for the univariate case $h(x) = x^k$. Equations 2.10 and 2.12 can also be derived from A3. For example, for the moments of Eqs. 2.12 we have, using the notation of Sec. 2:

$$\left\langle m^k \right\rangle_{q_j} = \int m^k q_j(m) dm = \int m^k m_j f(m) dm \qquad \text{(A4)}$$

and from A3:

$$\frac{d}{dt}\left\langle m^k \right\rangle_{q_j} = \int f(m) \frac{d}{dt}(m^k m_j) dm . \qquad \text{(A5)}$$

Equation 2.12 follows immediately on taking the derivative that appears in integral on the right hand side of A5.

Acknowledgements: This research was supported by NASA through interagency agreement number W-18,429 as part of its interdisciplinary research program on tropospheric aerosols and by the Environmental Sciences Division of the US Department of Energy, as part of the Atmospheric Chemistry Program under contract DE-AC02-76CH00016.

References

Abramowitz M. and Stegun I. A. (1972), *Handbook of Mathematical Functions* (Dover, New York) pg. 923.

Aris R. (1962), *Vectors, Tensors, and the Basic Equations of Fluid Mechanics* (Dover, New York) pg. 87.

Barrett J. C. and Webb N. A. (1998), A comparison of some approximate methods for solving the aerosol general dynamic equation, J. Aerosol Sci. 29, 31-39.

Barrett J. C. and Clement C. F. (1988), Growth rates for liquid drops, J. Aerosol Sci. 19, 223-242.

Capaldo K. P., Pilinis C., and Pandis S. N. (2000), A computationally efficient hybrid approach for dynamic gas/aerosol transfer in air quality models, Atmos. Environ. 34, 3617-3627.

Clegg S. L., Brimblecombe P., and Wexler, A. S. (1998), A thermodynamic model of the system $H^+ - NH_4^+ - SO_4^{-2} - NO_3^- - H_2O$ at tropospheric temperatures, J. Phys. Chem. A 102, 2137-2154.

Frenklach M. and Harris S. J. (1987), Aerosol dynamics modeling using the method of moments, J. Coll. Interface Sci. 118, 252-261.

Friedlander S. K. (1983), Annals of the New York Academy of Sciences 404, 354.

Friedlander S. K. and Wang C-S. (1966), The self-preserving particle size distribution for coagulation by Brownian motion, J. Coll. Interface Sci. 22, 126-132.

Hulburt H. M. and Katz S. (1964), Some problems in particle technology: A statistical mechanical formulation, Chem. Eng. Sci. 19, 555-574.

McGraw R. (1997), Description of aerosol dynamics by the quadrature method of moments, Aerosol Sci. and Technol. 27, 255-265.

McGraw R., Huang P. I. and Schwartz S. E. (1995), Optical properties of atmospheric aerosols from moments of the particle size distribution. Geophys. Res. Lett. 22, 2929-2932.

McGraw R., Nemesure S. and Schwartz S. E. (1998), Properties and evolution of aerosols with size distributions having identical moments, J. Aerosol Sci. 29, 761-772.

McGraw R. and Saunders J. H. (1984), A condensation feedback mechanism for oscillatory nucleation and growth, Aerosol Sci. Technol. 3, 367-380.

Meng Z., Dabdub D. and Seinfeld J. H. (1998), Size-resolved and chemically resolved model of atmospheric aerosol dynamics, J. Geophys. Res. 103, 3419-3435.

Pilinis C. (1990), Derivation and numerical solution of the species mass distribution equations for multicomponent particulate systems, Atmos. Environ. 24A, 1923-1928.

Pratsinis S. E. (1988), Simultaneous nucleation, condensation, and coagulation in aerosol reactors, J. Coll. Interface Sci. 124, 416-427.

Press W. H. and Teukolsky (1990), Orthogonal polynomials and gaussian quadrature with nonclassical weight functions, Computers in Physics, 423-426.

Press, W. H., Teukolsky, S. A., Vetterling W. T. and Flannery B. P. (1992), *Numerical Recipes in FORTRAN* (Cambridge University Press, Cambridge).

Tandon P. and Rosner D. E. (1999), Monte Carlo simulation of particle aggregation and simultaneous restructuring, J. Coll. Interface Sci. 213, 273-286.

Wang C-S (1966), *A mathematical study of the particle size distribution of coagulating disperse systems* (Doctoral Thesis, California Institute of Technology, Pasadena, California) pg 45.

Wolfram, S. (1999), *The Mathematica Book, 4th ed.* (Wolfram Media/ Cambridge University Press).

Wright D. L. (2000), Retrieval of optical properties of atmospheric aerosols from moments of the particle size distribution, J. Aerosol Sci. 31, 1-18.

Wright D. L., McGraw R., Benkovitz C. M. and Schwartz S. E. (2000), Six moment representation of multiple aerosol populations in a sub-hemispheric chemical transformation model, Geophys. Res. Letts. 27, 967-970.

Wright D. L., McGraw R. and Rosner D. E. (2001), Bivariate extension of the quadrature method of moments for modeling simultaneous coagulation and sintering of particle populations, J. Coll. Interface Sci., 236, 242-251.

Yoon C. and McGraw R. (2002), Multivariate extension of the quadrature method of moments for modeling generally-mixed particle populations, in preparation.

Yue G. K., Lu J., Mohnen V. A., Wang P.-H., Saxena V. K. and Anderson J. (1997), Retrieving aerosol optical properties from moments of the particle size distribution, Geophys. Res. Letts. 24, 651-654 (1997).

TABLE 1. Evolution of fractional 1/3 moments for the analytic test case of simultaneous condensation and coagulation with *H(m)*=1 and *K(u,v)*=1.

k	$\mu_k(t=0)$	$\mu_k(t=10)QMOM$	$\mu_k(t=10)exact$
0	1	22026.5	22026.5
1/3	1.19064	1.34451E6	1.33585E6
2/3	1.50458	8.63004E7	8.59850E7
1	2	5.82204E9	5.82198E9
4/3	2.77816	4.11311E11	4.11936E11
5/3	4.0122	3.027E13	3.03031E13

TABLE 2. Extension of the QMOM to the self-preserving limit. Results for constant and continuum-regime Brownian coagulation kernels. The table gives reduced moments ω_k from Eq. 5.12 and $\alpha = \omega_{1/3}\omega_{-1/3}/(1+\omega_{1/3}\omega_{-1/3})$. References are (a) Wang (1966), (b) Friedlander and Wang (1966).

k	$\omega_k(QMOM)$ *constant kernel*	$\omega_k(exact)$ *constant kernel* $=\Gamma(k+1)$	$\omega_k(QMOM)$ *Brownian kernel (continuum regime)*	$\omega_k(literature\ values)$ *Brownian kernel (continuum regime)*
0	1	1	1	1(a)
1	1	1	1	1(a)
2	1.99999	2	2.01022	2.014(a)
3	5.99992	6	6.05027	6.100(a)
4	23.9995	24	24.3116	24.77(a)
5	119.997	120	122.317	125.9(a)
α	0.52	0.547	0.52	0.53(b)

Figure Captions

Figure 1. Convergence of the total volume distribution $q(v) = vf(v)$ from the discrete representation of the distribution. Results are for evolution under continuum Brownian coagulation alone. Results from discrete representations employing 100, 200, 500, 1000, 2000, and 3000 grid points are shown. The upper panel shows the convergence of the initially normalized distribution itself, which is shown to be well represented even with 100 grid points. The lower panel shows the percent error differences between the discrete representation and the grid-independent QMOM result for the largest moment ($\mu_{5/3}$). Results are shown as a function of the number of grid points used in the discrete representation. Time is in reduced units, $\tilde{t}_{coag}$, defined in the text.

Figure 2. Moment evolution under simultaneous condensation and coagulation from the discrete representation (3000 grid points) and from the QMOM (dots). Results are shown for the total volume distribution $q(v)$ (solid line), and the species distributions $q_a(v)$ (bottom curve), $q_b(v)$ (second curve from bottom), and $q_c(v)$ (third curve from bottom). QMOM results with operator splitting are also shown for the total volume distribution $q(v)$ (diamonds) to access the influence of operator splitting used to obtain the benchmark results from the discrete representation. Time is in reduced units, $\tilde{t}_{coag}$, defined in the text.

Figure 3. Evolution of the dimensionless reduced moments ω_k for $k = 2 - 5$ for continuum Brownian coagulation alone (the values of ω_0 and ω_1 are by definition unity). Note the logarithmic time scale used to emphasize the approach to asymptotic behavior at comparatively short times.

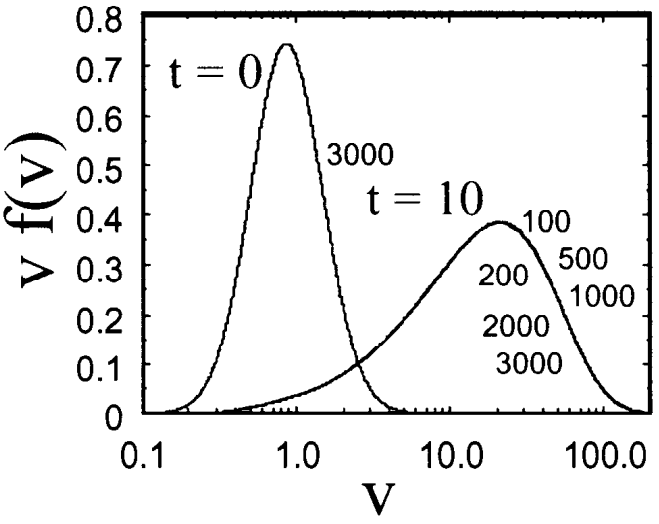
0.8
0.7
0.6
0.5
0.4
0.3
0.2
0.1
0
v f(v)
t = 0
3000
t = 10
100
500
200
1000
2000
3000
0.1
1.0
10.0
100.0
v

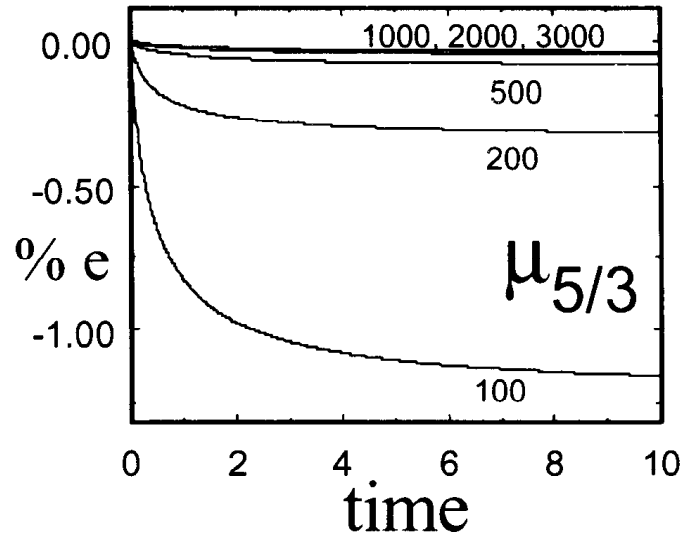
0.00
-0.50
-1.00
% e
1000, 2000, 3000
500
200
100
μ5/3
0
2
4
6
8
10
time

Figure 1

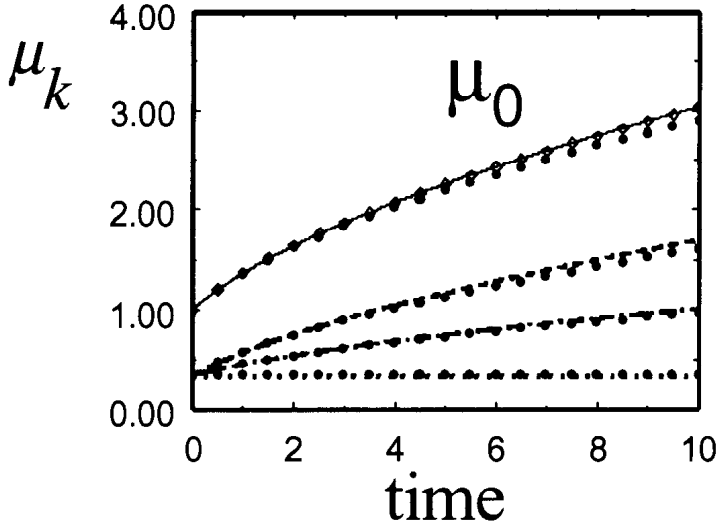
μ_k
4.00
3.00
2.00
1.00
0.00
μ_0
0
2
4
6
8
10
time

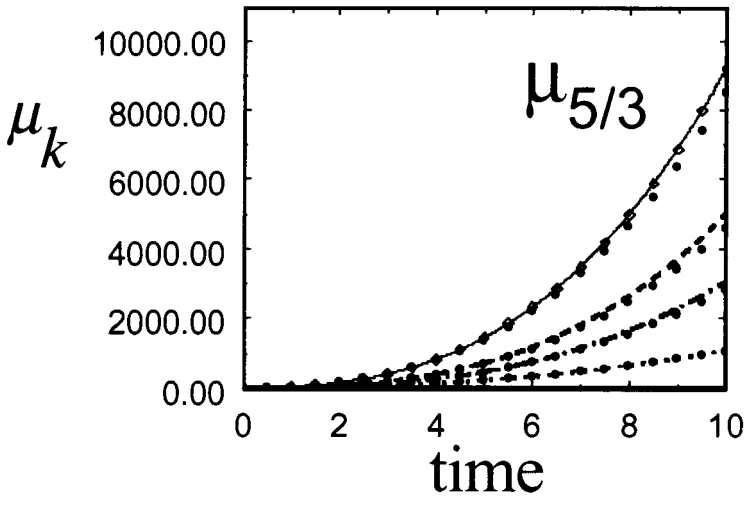
μ_k
10000.00
8000.00
6000.00
4000.00
2000.00
0.00
$\mu_{5/3}$
0
2
4
6
8
10
time

Figure 2

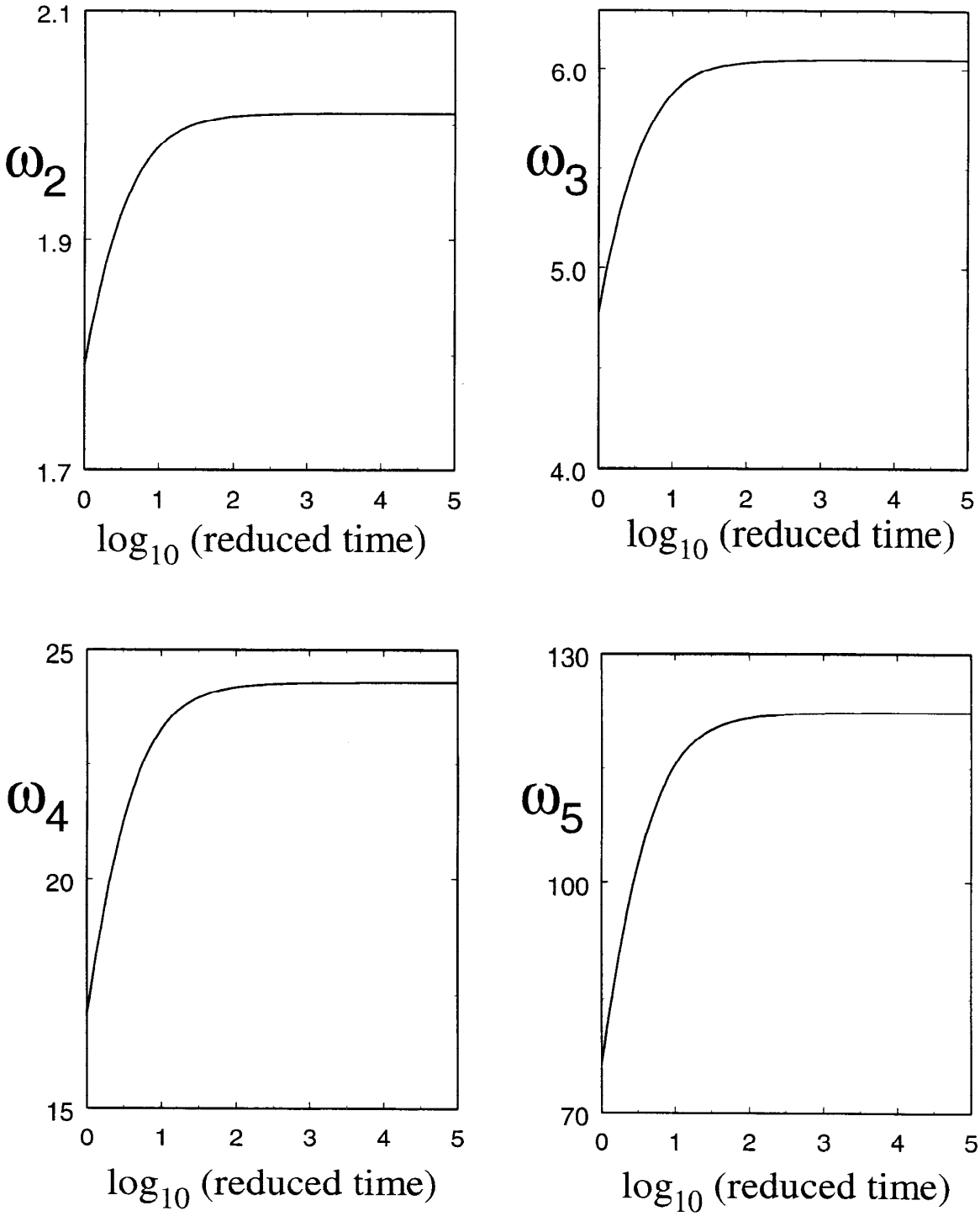
2.1
ω_2
1.9
1.7
0 1 2 3 4 5
$\log_{10}$ (reduced time)
6.0
ω_3
5.0
4.0
0 1 2 3 4 5
$\log_{10}$ (reduced time)
25
ω_4
20
15
0 1 2 3 4 5
$\log_{10}$ (reduced time)
130
ω_5
100
70
0 1 2 3 4 5
$\log_{10}$ (reduced time)

Figure 3